Available online at www.sciencedirect.com
ScienceDirect
Mendeleev Commun., 2011, 21, 221–223
Mendeleev Communications

Reaction characteristics of chemical-looping steam methane reforming over a Ce–ZrO_2 solid solution oxygen carrier

Xing Zhu,[a,b] Hua Wang,*[a,b] Yonggang Wei,[a,b] Kongzhai Li[a,b] and Xianming Cheng[a,b]

[a] *Faculty of Metallurgical and Energy Engineering, Kunming University of Science and Technology, 650093 Kunming, P. R. China*

[b] *Engineering Research Center of Metallurgical Energy Conservation and Emission Reduction, Ministry of Education, 650093 Kunming, P. R. China. Fax: +86 871 515 3405; e-mail: wanghuaheat@hotmail.com*

DOI: 10.1016/j.mencom.2011.07.017

The Ce–ZrO_2 solid solution oxygen carrier is active and stable in chemical-looping steam methane reforming for the co-production of syngas (synthesis gas) and hydrogen.

Chemical-looping steam methane reforming (CL-SMR) is a chemical looping derived technology.[1–4] In a CL-SMR process, methane is selectively oxidized to syngas (H_2:CO ratio of 2:1) by a suitable oxygen carrier; then, water is used to re-oxidize the oxygen carrier to produce hydrogen. Theoretically, syngas and pure hydrogen can be produced *via* this process as long as the oxygen carrier shows sufficient reactivity towards both reactants.[5,6]

The CL-SMR reactions are the following:

$$\text{Reduction: } M_xO_y + \delta CH_4 \rightarrow M_xO_{y-\delta} + \delta(2H_2 + CO), \quad (1)$$

$$\text{Oxidation: } M_xO_{y-\delta} + \delta H_2O \rightarrow M_xO_y + \delta H_2, \quad (2)$$

$$\text{Overall: } CH_4 + H_2O \rightarrow 3H_2 + CO, \quad (3)$$

where M and M_xO_y are a metal and an oxygen carrier (typically, a metal oxide), respectively, and $M_xO_{y-\delta}$ is the corresponding reduced oxygen carrier.

Steam methane reforming (SMR) is the most commonly used technology for large-scale hydrogen production.[7] However, conventional SMR is thermodynamically limited at high temperatures and pressures, and it requires a complex process for the purification of hydrogen.[8,9] In contrast, CL-SMR is a promising and attractive technology for methane conversion.

A disadvantage of CL-SMR is the insufficiently high temperature stability of oxygen carrier materials due to the weaker oxidizability of steam.[1] The application of ceria-based materials in industrial catalysis has attracted extensive attention.[10,11] A Ce–Zr–O solid solution exhibited a high structural stability in redox processes.[12–14] Though the selective oxidation of methane using the lattice oxygen of CeO_2 and Ce–ZrO_2 has been investigated,[12,13] the water splitting reaction involved in oxygen carrier regeneration and cycling redox performance has not been obtained.

Previously, we found that the Ce–Zr–O solid solution with a ceria content of ~70% has a good performance for the selective oxidation of methane.[15] The aim of this study was to investigate the performance of Ce–ZrO_2 solid solution (Ce:Zr ratio of 7:3) and CeO_2 oxygen carriers in CL-SMR.†

Figure 1 shows that, for both samples, CH_4 conversion increases rapidly and reaches a relatively steady state at ~50% in one minute. There is a fluctuation in the ascending curve of H_2 and CO selectivity due to the consumption of surface lattice oxygen (lower selectivity).[15] For the Ce–ZrO_2 sample, it shows a higher CH_4 conversion as soon as the reaction begins owing to the well releasing of bulk lattice oxygen in a Ce–Zr–O solid solution.[16] Because of the higher activity of lattice oxygen in the Ce–Zr–O solid solution, low selectivity for H_2 was found in the beginning of the reaction. The H_2:CO ratio rapidly increased with reaction time. Moreover, a higher specific surface area (40 $m^2\,g^{-1}$ for Ce–ZrO_2 *vs.* 21 $m^2\,g^{-1}$ for CeO_2) could also make a contribution to methane oxidation activity.[18]

Methane first reacted with active oxygen (surface absorption oxygen or surface lattice oxygen) to form CO_2 and H_2O during the gas-solid reaction between methane and oxides, and then bulk lattice oxygen (weaker lattice oxygen with high selectivity) could selectively convert methane into CO and H_2.[17] Thereafter, methane cracking ($CH_4 \rightarrow C + 2H_2$) would occur due to the lack

† The Ce–ZrO_2 complex oxide with a Ce:Zr ratio of 7:3 and pure CeO_2 were prepared by co-precipitation using sodium hydroxide instead of ammonia as the precipitator according to the procedure described previously.[16]

The powder X-ray diffraction (XRD) experiments were performed on a Japan Science D/max-R diffractometer using CuKα radiation (λ = = 0.15406 nm). The X-ray tube operated at 40 kV and 40 mA. Data were collected in the range of 2θ = 10–80 °C.

Temperature programmed reduction (TPR) experiments were performed on TPR Win v.1.50 (Quantachrome Instruments Co.) under a flow of a 10% H_2–He mixture (75 $cm^3\,min^{-1}$) over 100 mg of an oxygen carrier at a heating rate of 10 K min^{-1}.

The BET surface area was determined by N_2 physisorption using a Quantachrome NOVA 2000e sorption analyzer.

CL-SMR was carried out in a fixed-bed reactor under atmospheric pressure. An oxygen carrier (1.8 g) was placed in a quartz tube with an inside diameter of 20 mm. The oxygen carrier was predried in air at 300 °C for 2 h, and then pure N_2 was flowed to the reactor at 400 °C for 1 h. The reaction between methane (99.99% purity) and the oxygen carrier was performed at 850 °C. The total gas flow rate of methane was controlled by a mass flow controller at a specific flow rate of 10 $cm^3\,min^{-1}$ (NTP). Reactant and product components were analyzed on line using an Agilent 7890A gas chromatograph with a TCD and two capillary columns (HP-Plot 5A and HP-Plot-Q). After methane conversion, the reactor temperature was reduced to 700 °C and pure N_2 was used to purge the reactor for 30 min. Then, the water splitting reaction was initiated by introducing steam (with N_2 as a carrier gas at a flow rate of 50 $cm^3\,min^{-1}$) for 30 min. The steam was generated by injecting demineralized water in an electric furnace at 400 °C using a micro pump (0.18 $cm^3\,min^{-1}$).

The successive redox cycle measurement was also carried out in the fixed-bed reactor. Methane conversion and water splitting were performed at 850 and 700 °C, respectively. The conversion of CH_4 and the selectivity for CO and H_2 were found as described previously.[16,17] The reduction degree was calculated as amount of H_2 produced at step 2 (mol) divided by amount of oxygen atoms in oxygen carrier (mol).

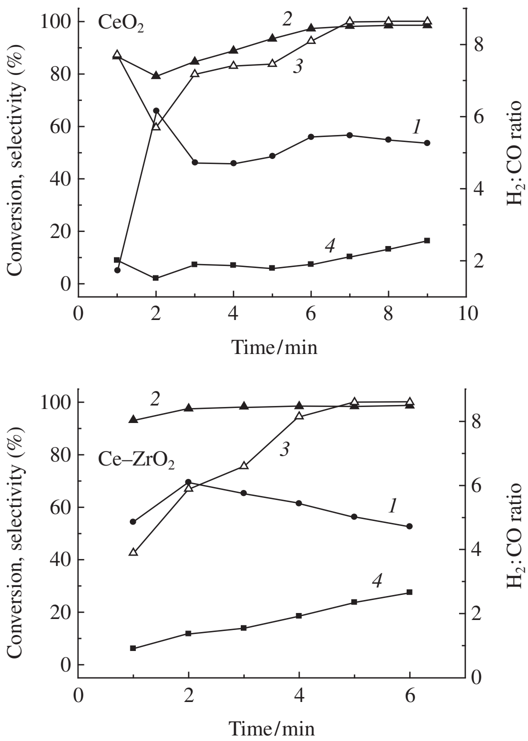

Figure 1 (*1*) CH_4 conversion, selectivity for (*2*) CO and (*3*) H_2, and (*4*) H_2/CO *vs.* reaction time at 850 °C over CeO_2 and Ce–ZrO_2 oxygen carriers in methane conversion reaction.

of lattice oxygen, which resulted in a high ratio of H_2:CO (>2). Since hydrogen will be contaminated by CO or CO_2 produced by carbon gasification, the reaction time for CeO_2 and Ce–ZrO_2 between methane should be controlled in 8 and 5 min, respectively, to avoid the formation of carbon deposit and to obtain a maximal reduction degree. In this situation, the degree of reduction of Ce–ZrO_2 at step 1 for chemical-looping cycles is 13.7%, which is twice as high as that of CeO_2.

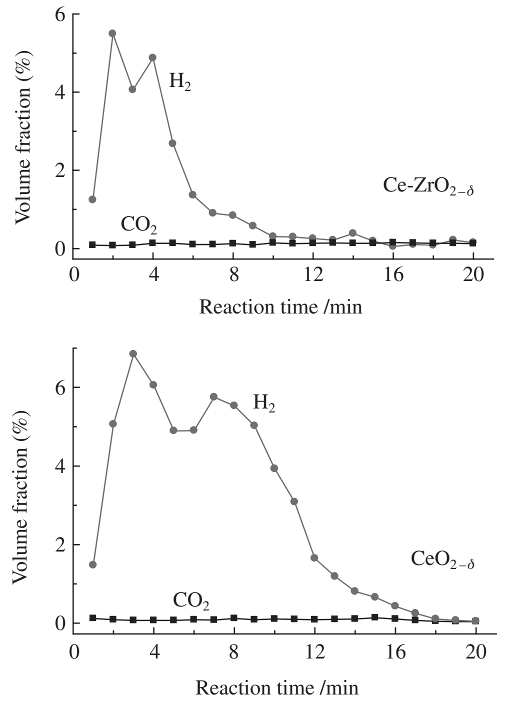

Figure 2 Product gas evolved volume fractions *vs.* reaction time in the water-splitting reaction over $CeO_{2-\delta}$ (with 8 min of reduction time at 850 °C) and Ce–$ZrO_{2-\delta}$ oxygen carriers (with 5 min of reduction time at 850 °C) at 700 °C.

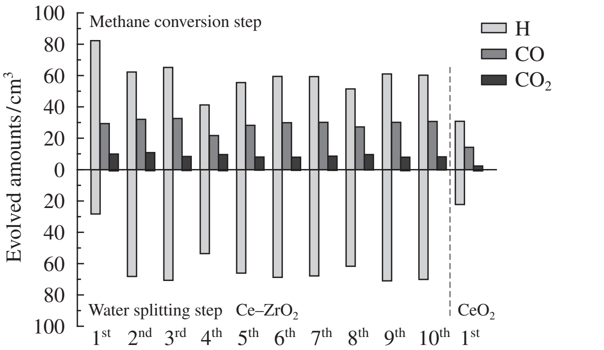

Figure 3 Evolved gas amounts in ten successive CL-SMR cycles over Ce–ZrO_2 oxygen carrier.

Figure 2 represents the hydrogen production profiles in water splitting reaction for $CeO_{2-\delta}$ and Ce–$ZrO_{2-\delta}$ samples. The H_2 volume fractions increase rapidly at the beginning of the reaction and then reach a high value in several minutes. Thereafter, they rapidly decrease to a near-zero level. The maximal formation rates of H_2 for $CeO_{2-\delta}$ and Ce–$ZrO_{2-\delta}$ were 2.9 and 3.6 cm^3 min^{-1} (corresponding to maximal volume fractions of 5.5 and 6.8%), respectively.

The bed temperature has an evident influence on water splitting reactivity.[19] Therefore, the hydrogen production rate fluctuates with the bed temperature. A similar phenomenon has been observed previously.[19] The Ce–$ZrO_{2-\delta}$ sample can supply more oxygen vacancies to generate more hydrogen in water splitting reaction.

Moreover, only a small amount of CO_2 (volume fraction of <0.24%) involved in H_2 was formed for both samples. These phenomena suggest that CO-free H_2 could be obtained in water splitting reaction over both samples, and the Ce–$ZrO_{2-\delta}$ sample shows a higher activity.

Figure 3 shows the amounts of gas produced over the Ce-ZrO_2 oxygen carrier in ten successive cycles. To restrain carbon deposition, the reaction times at step 1 for Ce–ZrO_2 and CeO_2 oxygen carriers were fixed at 5 and 8 min, respectively. Both the amounts of syngas and hydrogen over Ce–ZrO_2 are twice that of CeO_2 due to higher reduction degree, and no deactivation can be observed. The H_2:CO ratios of syngas produced at step 1 for nine cycles are in the range of 1.89–2.03, which is very close to an ideal value of 2.0. At step 2, only a negligible amount of undesired product CO_2 (volume fraction of <0.10%) was observed in the produced hydrogen.

The XRD patterns of Ce–ZrO_2 samples are represented in Figure 4. The fresh sample presents the peaks consistent with the formation of a Ce–Zr–O solid solution, with a cubic structure,[16] and they are slightly narrowed after the redox treatment, indicating an increased crystallization degree of the material. A weak peak at

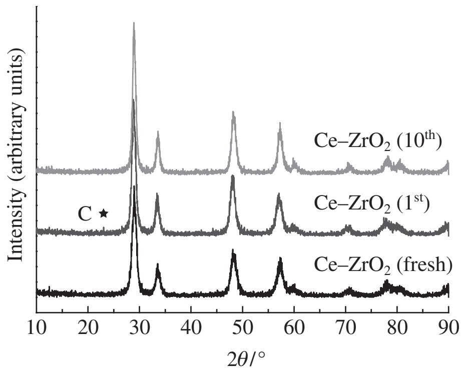

Figure 4 XRD patterns of a fresh Ce–ZrO_2 oxygen carrier and the carriers after the first and tenth cycles.

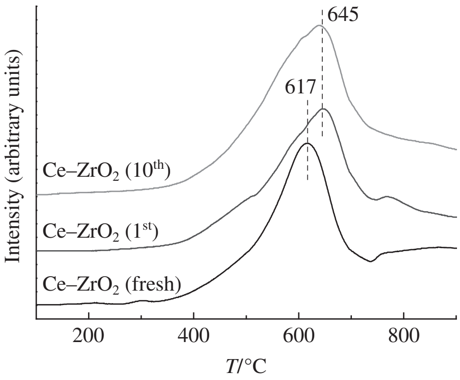

Figure 5 H_2-TPR patterns of a fresh Ce–ZrO_2 oxygen carrier and the carriers after the first and tenth cycles.

26.7° corresponding to carbon (marked by an asterisk in Figure 4) was detected in the Ce–ZrO_2 sample, but no carbon peak was detected in the sample after ten successive cycles. A possible explanation could be that the deposited carbon was removed by stream at the first cycle and no more evident carbon deposition formed thereafter.

The H_2-TPR patterns of fresh and recycled Ce–ZrO_2 oxygen carriers are shown in Figure 5. A broad peak at about 617 °C was attributed to the reduction of the uppermost layers of Ce^{4+} for the fresh sample. This peak slightly shifts to a higher temperature region (617 → 645 °C) after the high temperature redox cycles. This phenomenon should be ascribed to the sintering of the material, as observed by XRD measurements.

In summary, the Ce–ZrO_2 oxygen carrier exhibits good performance for the co-production of syngas and hydrogen using the chemical-looping steam reforming of methane due to the high structural stability and high reduction degree.

This work was supported by the National Natural Science Foundation of China (51004060), the Natural Science Foundation of Yunnan Province (2008E030M, 2010ZC108), the Research Foundation for the Doctoral Program of Higher Education of China (20095314120005), the Analysis and Test Foundation of Kunming University of Science and Technology (KUST), and the Innovation Foundation of KUST.

References

1 R. D. Solunke and G. Veser, *Ind. Eng. Chem. Res.*, 2010, **49**, 11037.
2 A. Steinfeld, P. Kuhn and J. Karni, *Energy*, 1993, **18**, 239.
3 K.-S. Kang, Ch.-H. Kim, K.-K. Bae, W.-Ch. Cho, S.-H. Kim and C.-S. Park, *Int. J. Hydrogen Energy*, 2010, **35**, 12246.
4 X. Zhu, H. Wang, Y. Wei, K. Li and X. Cheng, *J. Rare Earth*s, 2010, **28**, 907.
5 A. Evdou, V. Zaspalis and L. Nalbandian, *Int. J. Hydrogen Energy*, 2008, **33**, 5554.
6 A. Evdou, V. Zaspalis and L. Nalbandian, *Fuel*, 2010, **6**, 1265.
7 J. D. Holladay, J. Hu, D. L. King and Y. Wang, *Catal. Today*, 2009, **139**, 244.
8 K. S. Go, S. R. Son, S. D. Kim, K. S. Kang and Ch. S. Park, *Int. J. Hydrogen Energy*, 2009, **34**, 1301.
9 X. Zhu, H. Wang, Y. Wei, K. Li and D. Yan, *Proc. Int. Conf. on Power Engineering 2009 (ICOPE-09)*, 2009, vol. 2, p. 249.
10 A. A. Greish, L. M. Glukhov, E. D. Finashina, L. M. Kustov, J.-S. Sung, K.-Y. Choo and T.-H. Kim, *Mendeleev Commun.*, 2010, **20**, 28.
11 A. Trovarelli, C. de Leitenburg, M. Boaro and G. Dolcetti, *Catal. Today*, 1999, **50**, 353.
12 K. Otsuka, Y. Wang, E. Sunada and I. Yamanaka, *J. Catal.*, 1998, **175**, 152.
13 K. Otsuka, Y. Wang and M. Nakamura, *J. Catal.*, 1999, **183**, 317.
14 K.-S. Cha, H.-S. Kim, B.-K. Yoo, Y.-S. Lee, K.-S. Kang, C.-S. Park and Y.-H. Kim, *Int. J. Hydrogen Energy*, 2009, **34**, 1801.
15 K. Li, *Master's Degree Paper of Kunming University of Science and Technology*, 2008.
16 K. Li, H. Wang, Y. Wei and D. Yan, *Chem. Eng. J.*, 2010, **156**, 512.
17 K. Li, H. Wang, Y. Wei and D. Yan, *Appl. Catal. B: Environ.*, 2010, **97**, 361.
18 A. Trovarelli, F. Zamar, J. Llorca, C. de Leitenburg, G. Dolcetti and J. T. Kiss, *J. Catal.*, 1997, **169**, 490.
19 S. Abanades and G. Flamant, *Sol. Energy*, 2006, **80**, 1611.

Received: 11th January 2011; Com. 11/3658